

Free-piston batch reverse osmosis (RO)

Hosseini pour, Ebrahim; Davies, Philip

DOI:

[10.1016/j.desal.2024.117980](https://doi.org/10.1016/j.desal.2024.117980)

License:

Creative Commons: Attribution (CC BY)

Document Version

Publisher's PDF, also known as Version of record

Citation for published version (Harvard):

Hosseini pour, E & Davies, P 2024, 'Free-piston batch reverse osmosis (RO): Modelling and scale-up', *Desalination*, vol. 591, 117980. <https://doi.org/10.1016/j.desal.2024.117980>

[Link to publication on Research at Birmingham portal](#)

General rights

Unless a licence is specified above, all rights (including copyright and moral rights) in this document are retained by the authors and/or the copyright holders. The express permission of the copyright holder must be obtained for any use of this material other than for purposes permitted by law.

- Users may freely distribute the URL that is used to identify this publication.
- Users may download and/or print one copy of the publication from the University of Birmingham research portal for the purpose of private study or non-commercial research.
- User may use extracts from the document in line with the concept of 'fair dealing' under the Copyright, Designs and Patents Act 1988 (?)
- Users may not further distribute the material nor use it for the purposes of commercial gain.

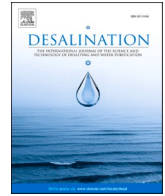
Where a licence is displayed above, please note the terms and conditions of the licence govern your use of this document.

When citing, please reference the published version.

Take down policy

While the University of Birmingham exercises care and attention in making items available there are rare occasions when an item has been uploaded in error or has been deemed to be commercially or otherwise sensitive.

If you believe that this is the case for this document, please contact UBIRA@lists.bham.ac.uk providing details and we will remove access to the work immediately and investigate.



Free-piston batch reverse osmosis (RO): Modelling and scale-up

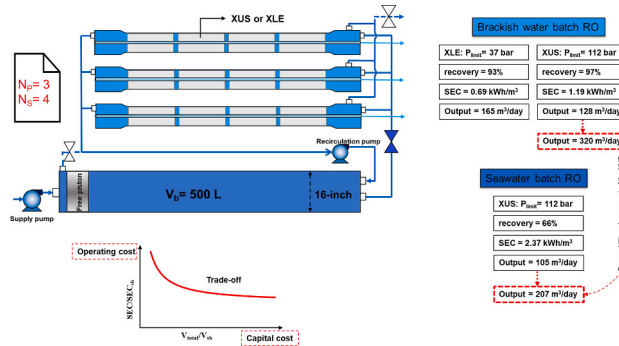
E. Hosseinipour^{*}, P.A. Davies^{*}

School of Engineering, University of Birmingham, Edgbaston, Birmingham, UK

HIGHLIGHTS

- Detailed model validation using brackish and seawater experiments up to 112 bar
- Batch RO scale-up: 12 membranes ($N_S = 4$ and $N_P = 3$) with a batch volume of 500 L
- 165 and 105 m³/day output with brackish and seawater, respectively
- SEC of 1.2 and 2.4 kWh/m³ at $r = 0.97$ and 0.66 with brackish and seawater at scale
- Improved permeability can nearly double output.

GRAPHICAL ABSTRACT



ARTICLE INFO

Keywords:

Batch RO
Scale up
High recovery
Energy efficiency
Membrane permeability

ABSTRACT

Free-piston batch RO achieves excellent energy efficiency at high recovery, but current systems have outputs <25 m³/day. Designing larger systems poses challenges like designing an appropriate work exchanger and optimizing membrane arrangements in series and/or parallel. This study calibrates a batch RO model against brackish and seawater experiments up to 112 bar and uses the model to predict performance on scale-up. Modelling up to 6 membranes in series predicts SEC of 1.11–1.5 kWh/m³ at recirculation flow $Q_r/Q_f = 4$ with brackish water, with SEC becoming more sensitive to Q_r/Q_f as the number of membranes increases. Using a 500-L work exchanger, a batch RO system with twelve 8-in. membranes is designed. For brackish water (3000 mg/L) this system gives outputs of 165 and 128 m³/day with SEC of 0.69 and 1.19 kWh/m³ at recoveries of 0.93–0.97 with low- and high-pressure RO membranes, respectively - representing SEC reductions of 33 and 45 % compared to semi-batch RO. For seawater, it gives 105 m³/day with SEC of 2.37 kWh/m³ at recovery of 0.66. High-permeability membranes would significantly enhance batch RO performance; for example, increasing permeability from 0.8 to 2 L/m²/h/bar would boost output to 320 and 207 m³/day in brackish and seawater desalination respectively.

1. Introduction

Reverse osmosis (RO) stands out as one of the most

thermodynamically effective and economically viable methods for desalination [1,2]. Among RO configurations, batch RO is an innovative approach noted for its high energy efficiency, particularly at high recovery [3]. This makes it especially interesting for minimal or zero

^{*} Corresponding authors.

E-mail addresses: e.hosseinipour@bham.ac.uk (E. Hosseinipour), p.a.davies@bham.ac.uk (P.A. Davies).

<https://doi.org/10.1016/j.desal.2024.117980>

Received 22 May 2024; Received in revised form 25 July 2024; Accepted 4 August 2024

Available online 8 August 2024

0011-9164/© 2024 The Authors. Published by Elsevier B.V. This is an open access article under the CC BY license (<http://creativecommons.org/licenses/by/4.0/>).

Nomenclature			
Symbols		Q_f	L/min, Feed flow from high-pressure supply pump
A_w	L/m ² /h/bar, Membrane permeability	Q_r	L/min, Recirculation flow at brine outlet of RO module
A_m	m ² , Membrane area	r	-, Water recovery
C_d	-, Coefficient of discharge	R_s	-, Salt rejection
c_{feed}	mg/L, Feed concentration	V_b	L, Swept volume of work exchanger
D	mm, Pipe diameter	V_h	L, Volume of the pressure vessels housing the membranes
f	-, Friction factor	V_{total}	L, Total volume of pressure vessels comprising membrane housings and the work exchanger
J_w	L/m ² /h, Flux	v	m/s, Cross-flow velocity
L	-, Pipe length	ρ	kg/m ³ , Density
L_m	m, Membrane length	Abbreviations	
N_d	-, Number of equivalent diameters added to unpurged section to represent minor losses	MLD/ZLD	Minimal/Zero Liquid Discharge
N_p	-, Number of elements in parallel	RO	Reverse Osmosis
N_s	-, Number of elements in series	SEC	Specific Energy Consumption
ΔP_m	kPa, Cross-flow pressure drop across RO membrane	SI	Supporting Information
$\Delta P_{orifice}$	kPa, Pressure drop across orifice	XLE	Membrane (FilmTec™ BW XLE-440)
$\Delta P_{recirc,pipe}$	kPa, Pressure drop across pipe	XUS	Membrane (Dupont XUS180808)

liquid discharge (MLD/ZLD) applications [4–6] and for brackish water desalination [7–10]. There is a growing interest in MLD/ZLD, particularly for decentralized water treatment [11–13]. Applications include treatment of wastewater from metal plating [6], textile industry [14], semiconductor industry [15], food processing industries [16,17], hydroponic waste recycling [18], and mineral recovery such as lithium extraction [19–22]. Recent literature underscores the increasing needs to enhance water and solute recovery and extract valuable metals and chemicals from wastewater and desalination concentrates [23–25]. Batch RO systems could play a significant role in these areas. Developing innovative approaches, such as batch RO, is crucial to meet these needs, especially given the European Union's strategic priorities such as water resilience and circular economy [26]. So far, however, research in batch RO has been mostly limited to small-scale laboratory studies, where the output is <25 m³/day. Even in decentralized water treatment applications, capacities of 1000 m³/day or larger may be required. Therefore, there is a need to address the challenge of scaling up batch RO.

Unlike continuous RO, batch RO recovers water in multiple passes achieving more uniform flux distribution over the membrane [27–30]. In ideal batch RO, there is no spatial variation in quantities of flux, concentration or osmotic pressure; thus, the lowest thermodynamic energy consumption is theoretically possible [3,31]. In reality, however, these quantities do vary somewhat over the RO membrane element, reducing the energy savings [8,32]. This problem is minimized by decreasing the recovery per pass, i.e., by increasing the recirculation flow [8,33]. However, scale up of batch RO is likely to need several membrane elements in series, which may aggravate losses associated with the recirculation flow. On the one hand, use of several elements in series is beneficial in reducing the number of vessels and amount of pipework. On the other hand, it requires an increased recirculation flow to maintain uniform flux, incurring higher energy consumption [34]. Thus, there is a trade-off between a simpler, low-cost design and a design that is more energy efficient [33]. In semi-batch RO applications, 3–4 membrane elements in series have been favoured [35–37], as opposed to 6–8 typically used in conventional continuous RO plants. For batch RO, however, experimental reports have so far been limited to just one element per vessel. Consequently, it is important to quantify batch RO performance with multiple elements in series to meet the scale up challenge.

The main approaches to batch RO use either: (1) atmospheric vessels with energy recovery devices, or (2) pressurized work exchanger vessels. In a theoretical study based on the first approach, Das et al. [38] introduced a design for zero downtime and scalability. They simulated

such a design comprising five parallel trains each having five membranes in series (a total of 25 membranes), to predict a plant capacity of 378.5 m³/day with seawater feed (35,000 mg/L NaCl). Key assumptions included membrane permeability of 3 L/m²/h/bar, high recovery ratio per pass of 0.45, salt rejection of 99.4 %, pump efficiencies of 80 %, and a membrane pressure rating of 83 bar. The study calculated Specific Energy Consumption (SEC) of 2.12 kWh/m³ (corresponding to a 2nd law efficiency of 48.2 %) and overall system recovery of $r = 0.51$. Despite such favourable results, the study concluded that the proposed system still consumes ~7.6 % more energy than designs using pressurized work exchangers at the conditions specified above. Free-piston batch RO design is one such design [3,8].

Davies et al. [3] reported the first experimental study of free-piston batch RO. They constructed a prototype using readily available components and tested it with varying feed salinities (2000 to 5000 mg/L) and recovery ratios (0.17 to 0.71). The prototype consisted of one pressure vessel (i.e., work exchanger) housing free pistons of different lengths to vary the recovery, and two pressure vessels in parallel each housing one 2.5-in. diameter membrane element (FilmTec™ BW30 with area of 2.6 m²). The tests were conducted at fluxes of 7–23 L/m²/h, resulting in output of 0.9–2.6 m³/day. A limitation of this prototype was the interruption of output while the system refilled between cycles. Thus, this group designed a new configuration in which the work exchanger is double-acting, i.e., one side refills while the other side pressurizes. This allowed continuous output during the refill phase and boosted water production by about 25 % compared to the earlier design, without increasing membrane area [7]. However, the double-acting arrangement was considered somewhat complex requiring 5 valves and 3 pumps. Therefore, this group opted instead to pursue a single-acting arrangement that combined the purge and refill stages to minimize downtime, while requiring only 3 valves and 2 pumps (see Fig. 1) [39].

Another type of pressurized work exchanger employs a flexible bladder instead of a free piston. Wei et al. [30] designed and operated the first bladder batch RO. In their bench-scale prototype, they used a single pressure vessel to house both the bladder and membrane (Hydranautics ESPA-2514 with the membrane area of 0.47 m²). They conducted their experiments at recovery <0.55 (due to a pressure limit of 10 bar), feed salinities of 2000–5000 mg/L and fluxes of 10–20 L/m²/h, giving an output of 0.1–0.2 m³/day.

Park et al. [8] designed a larger free-piston batch RO using an 8-in. RO membrane, intended for brackish water desalination at recovery of $r = 0.8$. This design was later constructed and tested with various feed

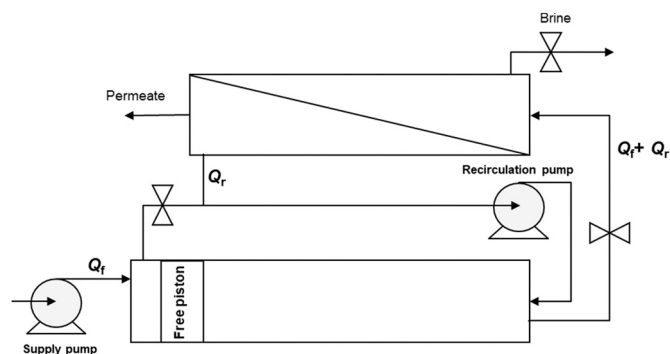


Fig. 1. Schematic of a single-acting free-piston batch RO showing supply flow Q_f and recirculation flow Q_r .

solutions including NaCl solution [9,40] and synthetic brackish groundwater [10] at different water fluxes (11–23 L/m²/h) using 5 different membrane types each with the surface area of 41 m². Output up to 22 m³/day was achieved. Subsequent studies introduced the concept of hybrid semi-batch/batch RO which was designed to avoid the need for excessively large work exchangers at recoveries >0.8 [4,5]. Following these studies, a high-pressure (120 bar) hybrid semi-batch/batch RO pilot was designed for the treatment of metal plating wastewater [6]. This pilot was also used to carry out the first direct experimental comparison of batch RO technologies [41]. A high-pressure membrane (Dupont XUS180808) with active area of 30.6 m² was used at fluxes <17 L/m²/h in this pilot, giving outputs up to 12 m³/day. In summary, experimental studies of batch RO to date had outputs of only 0.1–22 m³/day (see Table 1).

The scale of RO systems can vary greatly depending on specific application needs, environmental regulations, and feedwater sources. The choice of scale for a project is influenced by factors such as population served, industrial demand, environmental constraints, and economic feasibility. For example, in reviewing brackish water desalination systems, Zhao et al. reported a wide range of capacities from 0.2 to 25,000 m³/day [42].

Whereas the approach to scaling up conventional RO plants is well established, this is not the case for batch RO where several new issues arise. One issue relates to the need for a large work exchanger vessel (in the case of the free-piston or bladder design), especially at recoveries above about $r = 0.8$ [4,5,30]. For example, achieving a recovery of $r = 0.95$ through pure batch operation needs a work exchanger volume of approximately 300 L for each 8-in. membrane. This translates to an excessive length of 9 or 4.5 m when employing an 8-in. or 16-in. diameter vessel, respectively, for the work exchanger. This would greatly increase the footprint and capital cost of the system.

Table 1

Experimental studies of batch RO and their output volumes.

Work exchanger type	Year	Membrane area (m ²)	Approximate output (m ³ /day)	Notes	References
Free-piston (single acting)	2016	2 × 2.6	0.9–2.6	The recovery ranged from 0.17 to 0.71, with the brackish feed water varying between 2000 and 5000 mg/L. Hydraulic SEC was reported.	[3]
Free-piston (double acting)	2016	8.7	3.2	Increased water production by 25 % compared to the single-acting design. The recovery ranged from 0.7 to 0.8 when using brackish water.	[7]
Free-piston (single acting)	2018	3 × 2.6	3.8	The recovery achieved was 0.72 when using brackish water with a feed concentration of 2000 mg/L.	[39]
Bladder (low pressure)	2020	0.47	0.1–0.2	The recovery ranged from 0.3 to 0.5 when using brackish water with feed concentrations ranging from 2000 to 5000 mg/L. Hydraulic SEC was reported the pressure limit of the system was 10 bar.	[30]
Free-piston (low pressure)	2022	41	10–22	The recovery ranged from 0.8 to 0.95 when using brackish water with feed concentrations ranging from 500 to 5000 mg/L. Electrical SEC of 0.4 to 0.8 kWh/m ³ was reported. The pressure limit of the system was 25 bar.	[5,9,10,40]
Free-piston (high pressure)	2023	30.6	4–12	Recovery of 0.85 to 0.96 with brackish and seawater feed as well as electroplating wastewater. Electrical SEC < 3.5 kWh/m ³ was reported. The pressure limit of the system was 120 bar.	[6,41]

Additionally, longer pressure vessels increase the risk of inadequate mixing between the recirculating brine solution and the feed solution in the work exchanger, potentially leading to performance loss or necessitating higher recirculation flow and thus increasing SEC. This problem has been partially overcome with the introduction of hybrid semi-batch/batch RO, as noted above [4].

Another issue regards the pipework. In conventional RO, the layout and sizing of pipework are not critical, provided it is adequately sized to avoid frictional resistance which would otherwise increase the pumping energy. In batch RO, however, retention of salt from one cycle to the next makes it important to avoid oversizing [8,9,28,30]. Therefore, the pipework must be optimised considering this trade-off between minimizing salt retention and flow resistance. For larger plants, which tend to require longer pipe runs, this trade-off may become more important.

Thus, in this study, the aim is to accurately predict scaled up performance of batch RO based on the single-acting free-piston design as described in [4,8] (see Fig. 1). This will be done with careful validation against a laboratory prototype rated at 120 bar. Using hybrid semi-batch/batch operation, water recovery up to $r = 0.97$ is achieved. Thus, the study will give a complete and reliable picture about scaling up free-piston batch RO, providing a guide for design selection and optimisation at outputs up to about 300 m³/day which is >10 times larger than currently implemented.

2. Model development

The model presented in this paper has been developed by modifying an existing model to reflect features that are important in the scale up of the system.

2.1. Overview of existing model

The model was developed through several iterations alongside the development of free-piston batch RO in Birmingham, UK. Recently, it has been validated against two prototypes at the University of Birmingham. The model initially developed by Park et al. [8] included most losses and led to a specific design recommendation for brackish water treatment. However, in experimental studies of the recommended design, Hosseini-pour et al. [9] identified osmotic backflow (previously neglected) as an additional loss which they therefore incorporated into the model.

The next step was the development of hybrid semi-batch/batch RO, used to achieve recovery >0.8 in a compact design. As with the non-hybrid batch RO, the initial model [4] of the hybrid system did not consider osmotic backflow and therefore had to be modified to include it. Also, at very high recoveries, the assumption of 100 % salt rejection was no longer a good approximation in calculating salt retention, peak

pressure, and *SEC*. Thus, the modelling of salt retention was improved by adjusting for salt rejection, thus predicting *SEC* with <3 % error [5].

Further features of the modelling included representation of the longitudinal concentration gradient in the RO module by a linear approximation whereby the average concentration is assumed equal to the average of inlet and outlet concentrations [4,5,8,9]. The typically high recirculation rate in the module (giving recovery per pass <33 %) results in only a small increase in the applied pressure relative to the idealised case of infinite recirculation flow, thus justifying the approximation. The approach avoids the need to solve partial differential equations representing the non-steady behaviour of the batch RO system, which depends on both space and time variables. Instead, only explicit algebraic equations are used.

For a complete description of the existing model, the reader is referred to the works referenced above.

2.2. Modifications for frictional pressure losses affecting recirculation pump

On scaling up, the recirculation flow tends to increase, amplifying frictional pressure losses, and increasing the energy consumption of the recirculation pump. Some modifications have been made to the model to ensure that these losses are represented with sufficient accuracy. Frictional pressure losses depend on the flow path according to the phase of operation (see Fig. S1 and Table S1).

Pressure drop ΔP_m [kPa] along the membrane channel is caused by friction with the membrane surface and spacer element. As in our previous studies [4,5,8,9], the correlation (Eq. (1)) established by Haidari et al. [43] is employed for ΔP_m .

$$\Delta P_m = k \times v^{1.63} \times L_m \quad (1)$$

where v is the cross-flow velocity [m/s], and L_m [m] is the length of the membrane. Haidari used a constant k value of 791 but this has been modified based on experimental measurements in the current study. The cross-flow velocity was averaged between inlet and outlet.

The longest pipe section in the free-piston batch RO system is that either side of the recirculation pump, highlighted in red Fig. 5. In the current prototype at the University of Birmingham, this section has a length of 2.2 m. For scale up, to match the total membrane length, we added 1 m for each additional membrane element, such that the length becomes 7.2 m for 6 membranes in series. This length is important regarding both salt retention and pressure loss. Other pipe sections are <0.5 m in length, so for those shorter sections, pressure losses are calculated by considering them equivalent to an orifice of the same diameter as the internal diameter of the pipe. In this way, the exit loss from the pipe was represented. The pipe friction is calculated using a friction factor of $f = 0.024$ and an additional pipe length (L) equivalent to $N_d = 75$ times the pipe diameter ($D = 21.2$ mm in the case of the existing pilot) is allowed for the total minor losses in bends and fittings. Thus, the equation for pressure drop in the recirculation pipe is:

$$\Delta P_{\text{recirc,pipe}} = \frac{f(L + N_d \cdot D)}{D} \frac{\rho v^2}{2} \quad (2)$$

Friction factor may depend on Reynolds number (Re) which, in this study, ranged from about 50,000 to 150,000. Nonetheless, as there is only a weak dependency on Re (typically following the Blasius equation $f = 0.31 Re^{-0.25}$) a constant value of f was adopted for simplicity. The diameter D was also increased on scale up. It was optimised by trial-and-error while selecting from standard available diameters.

The Torricelli equation for flow through an orifice is used to represent pressure drop through valves or short pipe lengths, as follows:

$$\Delta P_{\text{orifice}} = \frac{\rho}{2} \left(\frac{v}{C_d} \right)^2 \quad (3)$$

where v represents the velocity at the orifice, and C_d denotes the

coefficient of discharge. As noted by Massey [44], C_d typically falls within the range of 0.6 to 0.7 and is adjusted to $C_d = 0.62$ in the model.

3. Model validation

Model validation measurements were carried out using the single-acting free-piston batch RO system and a DuPont XUS180808 membrane rated at 120 bar (henceforth referred to as XUS). The experimental equipment and method were as described previously [6,41]. NaCl solution was used as feed.

3.1. Frictional pressure losses affecting recirculation pump

We conducted experiments to measure the pressure across the recirculation pump, at 4 different recirculation flows and over three phases of operation, giving 12 measurements in total. After adjusting three parameters (i.e., k in Eq. (1), the piston seal friction pressure, and the friction factor, f , in Eq. (2)) we arrived at the modelling results in Table 2 which agree with the measured pressure drop with 0.5 to 7 % error.

Though the value of $k = 300$ used for the XUS membrane differs significantly from the value of $k = 791$ used by Haidari et al. [43], we also observe a wide variation in the literature. For example, FilmTec™ RO membranes technical manual provides a value of $k = 450$ but without reference to any specific type of membrane [45]. Moreover, for membrane elements with thinner feed spacers, we experimentally observed higher values, such as $k = 600$ for FilmTec™ BW XLE-440 (with feed spacer thickness of 28 mil compared to 34 mil for the XUS; see Table S2 for the membrane properties taken from the manufacturer's datasheet). Using real data from a seawater desalination plant located in the Persian Gulf having 7 membranes in series in each pressure vessel and operating at the recovery of $r = 0.4$ and flux of 15 L/m²/h, this value was about $k = 370$ (with feed spacer thickness of 34 mil). Therefore, we consider that the value of $k = 300$ is reliable for the XUS membrane.

3.2. Overall SEC

Having established the modelling of pipework losses, we next validate the whole system modelling for *SEC* taking into account membrane properties. This part of the modelling uses two additional adjustable parameters: (1) membrane permeability, adjusted to 0.8 L/m²/h/bar and (2) salt rejection R_s adjusted to 0.985 and 0.96 for seawater and brackish water respectively, which was consistent with the experimental values.

In the case of a seawater feed, the experimentally measured hydraulic *SEC* matched closely the model prediction, with <3 % error observed across various fluxes at recovery $r = 0.63$ (Fig. 2). For brackish water feed, the corresponding error was <4 % (Fig. 3) based on tests at the flux of 16.8 L/m²/h and recovery of $r = 0.952$ (except at $c_{\text{feed}} = 5000$ mg/L when recovery was 0.942 due to the peak pressure limit).

3.3. Effect of recirculation flow

Recirculation flow is quantified as the ratio Q_r/Q_f of the flow at the brine outlet divided by the feed flow from high-pressure supply pump (see Fig. 1). In a prior investigation [5], we examined the effect of recirculation flow in a low-pressure hybrid RO system in treating low-concentration NaCl solutions ($c_{\text{feed}} = 1000$ mg/L). To minimize *SEC*, we optimised the recirculation flow as $Q_r/Q_f = 2$ (equivalent to a recovery per pass of 0.33). Here, we conducted a similar experiment to optimise Q_r/Q_f in the high-pressure system using values of $Q_r/Q_f = 2.3, 4.1$ and 5.7 (corresponding to the recovery per pass of 0.15–0.3) at $c_{\text{feed}} = 4000$ mg/L, $J_w = 16.8$ L/m²/h, and $r = 0.954$.

On increasing the recirculation flow while maintaining the feed flow at 8.8 L/min (i.e. increasing Q_r/Q_f) peak pressure decreased uniformly, whereas the total *SEC* initially decreased and then increased (Fig. 4A).

Table 2

Comparison of experimental results and modelling predictions for the recirculation pump pressure drop over 3 phases of operation in the free-piston batch RO when using the XUS membrane. Parameters of $k = 300$ for the RO membrane pressure drop, piston friction pressure drop of 25 kPa, and pipe friction factor of $f = 0.024$ were used in the modelling.

Feed salinity (mg/L), c_{feed}	Recovery, r	Flow (L/min)		Recirculation pump pressure drop (kPa)						Hydraulic SEC			
		Supply pump, Q_f	Recirc pump, Q_r	Experimental results			Modelling results (% of deviation)			Experimental results		Modelling results (% of deviation)	
				Semi-batch	Batch	Purge-and-refill	Semi-batch	Batch	Purge-and-refill	Supply pump	Recirc pump	Supply pump	Recirc pump
4000	0.95	8.7	20	6.9	5.6	43.4	7.4 (6.7 %)	5.3 (5.7 %)	43.1 (0.7 %)	1.298	0.007	1.250 (3.8 %)	0.008
5000	0.94	6.1	23.3	7.5	6.3	42	7.9 (5.1 %)	6.3 (0 %)	42.6 (1.4 %)	1.067	0.010	1.020 (4.6 %)	0.012
5000	0.95	6.1	27.5	10.2	8.7	42	10.2 (0 %)	8.4 (3.6 %)	42.8 (1.9 %)	1.165	0.015	1.105 (5.4 %)	0.017
4000	0.95	8.7	36	17.1	16.4	43.3	17.7 (3.4 %)	15.3 (7.2 %)	43.1 (0.5 %)	1.209	0.026	1.164 (3.9 %)	0.026

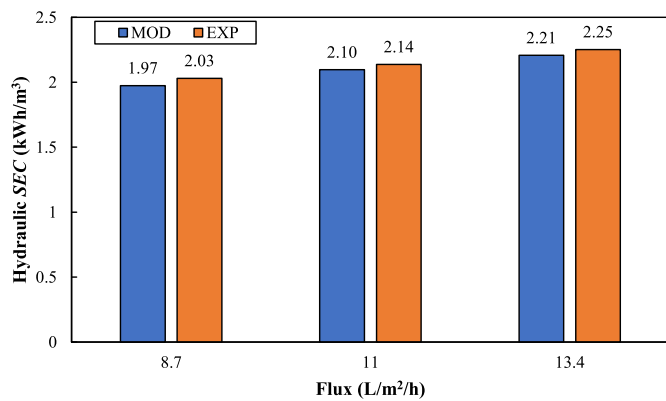


Fig. 2. Comparison of model predictions (MOD) and experimental measurements (EXP) of hydraulic SEC for seawater feed at recovery of $r = 0.63$ (XUS membrane). Experiments were conducted exclusively in batch mode because the recovery is low due to the high osmotic pressure of the feed, avoiding the need for the hybrid mode.

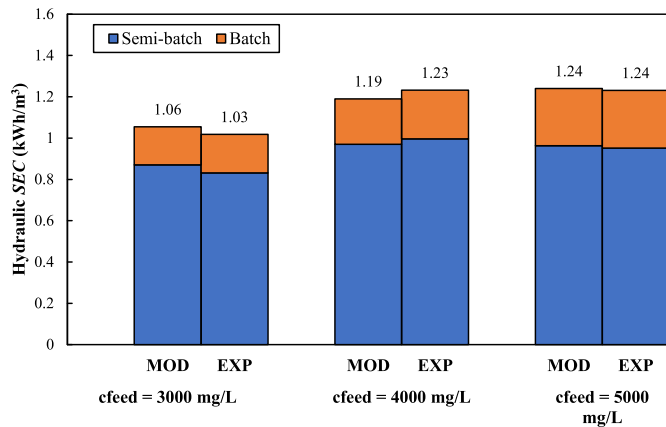


Fig. 3. Comparison of model predictions (MOD) and experimental measurements (EXP) of hydraulic SEC at different feed concentrations, $J_w = 16.8$ L/m²/h, and recovery of $r = 0.952$ (except for $c_{\text{feed}} = 5000$ mg/L where $r = 0.942$). XUS membrane was used. Experiments were conducted in hybrid semi-batch/batch mode because achieving such a high recovery with a batch RO would require an impractically large work exchanger (approximately 300 L compared to the 40 L used here).

For example, the peak pressure fell from 108 to 102 and then 100 bar, on increasing Q_r/Q_f from 2.3 to 4.1 and then 5.7 respectively; while hydraulic SEC decreased from 1.30 to 1.24 kWh/m³ initially and then increased again to 1.27 kWh/m³ (Fig. 4B). The main reason for the

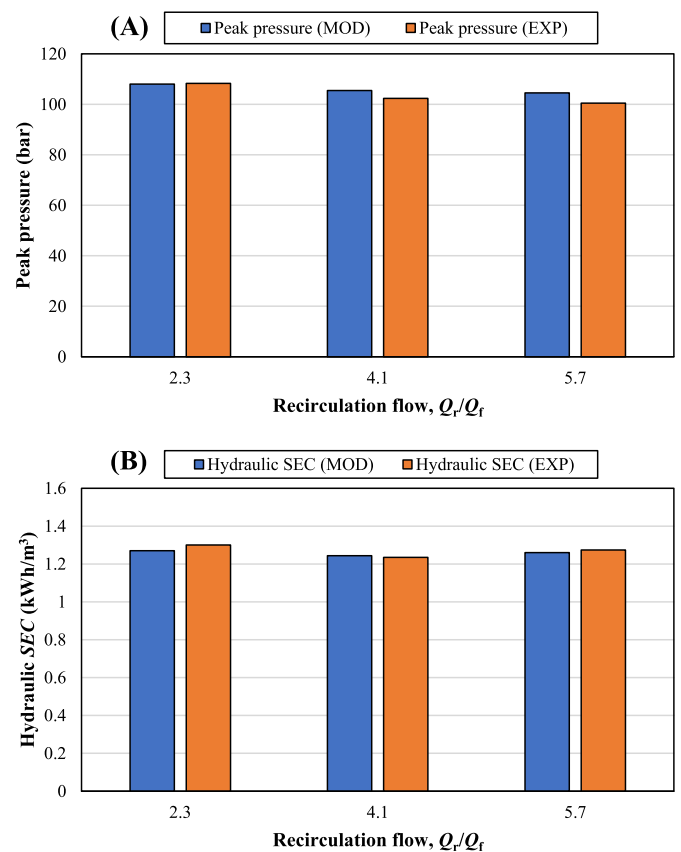


Fig. 4. Comparison of the model predictions (MOD) and experimental measurements (EXP) when varying the recirculation flow, A) peak pressure, and B) hydraulic SEC. Brackish water: $c_{\text{feed}} = 4000$ mg/L, $r = 0.954$ and $J_w = 16.8$ L/m²/h. Hybrid semi-batch/batch RO operation.

decreased peak pressure is that the recirculation flow promotes a uniform concentration in the feed channel transversally and longitudinally (i.e., decreasing the concentration polarization and longitudinal concentration gradients) which in turn decreases the required applied pressure (see also Table 3). In turn, this reduces the energy consumption of the supply pump. However, on increasing Q_r/Q_f , the recirculation pump energy consumption increases (Table 3). Hence there is a trade-off between supply pump energy saving and recirculation pump energy saving. Increasing Q_r/Q_f also improved permeate quality, reducing conductivity by 11 % when almost doubling Q_r/Q_f . The model predicted hydraulic SEC and peak pressure within 4 % of the above experimental values (Fig. 4).

Priorities of specific applications will determine the preference

Table 3

Experimental measurement of the effect of varying Q_r/Q_f ratio on the main parameters of the high-pressure free-piston batch RO including permeate quality, average pressure and SEC. Brackish water $c_{\text{feed}} = 4000 \text{ mg/L}$, $r = 0.954$ and $J_w = 16.8 \text{ L/m}^2/\text{h}$.

Q_r/Q_f	Permeate conductivity (mS/cm)	Rejection, R_s	Average applied pressure (bar)	Peak pressure (bar)	Hydraulic SEC (kWh/m ³)	Electrical SEC (kWh/m ³)		
						Supply pump	Recirc pump	Total
2.3	0.351	0.957	45.9	108.3	1.30	2.01	0.04	2.05
4.1	0.324	0.960	42.7	102.3	1.24	1.91	0.08	1.99
5.7	0.310	0.962	41.9	100.4	1.27	1.89	0.16	2.05

between achieving a slightly lower peak pressure with slightly higher energy consumption (operating at Q_r/Q_f approximately 5 to 6) or slightly lower energy consumption with a higher peak pressure (operating at Q_r/Q_f around 4).

4. Model predictions

Following the above validation and optimisation, this section uses the model to predict and optimise scale up for brackish and seawater feed. Table 4 shows baseline parameters used by default, as well as variations used in the scaled-up modelling.

4.1. Effect of work exchanger size

As mentioned in Section 2, it is important to consider the size of the

Table 4

Parameters for the free-piston batch RO modelling, showing baseline (default) values and variations used for scale up (brackish and seawater feed).

Parameter	Brackish water feed		Seawater feed	
	Baseline	Scale up	Baseline	Scale up
Feed salinity, c_{feed} (mg/L)	3000	3000	35,000	35,000
Water recovery, r	0.97	0.93 and 0.97	0.66	0.66
Average water flux, J_w (L/m ² /h)	15	15	15	15
Membrane type	XUS	XUS, XLE	XUS	XUS
Number of elements in series, N_s	1	1–6	1	1–6
Number of elements in parallel, N_p	1	1–3	1	1–3
Total membrane area, A_m (m ²)	30.6	30.6 and 492	30.6	30.6 and 367.2
Membrane water permeability, A_w (L/m ² /h/bar)	0.8	0.8 and 4.6	0.8	0.8
Salt rejection, R_s	0.96	0.92 and 0.96	0.98	0.98
Q_r/Q_f (or recovery per pass ratio)	4 (0.2)	2 (0.33)–8 (0.11)	4 (0.2)	2 (0.33)–8 (0.11)
Supply (high-pressure) and recirculation pumps efficiency (%)	80	80	80	80
k value for membrane pressure drop (Eq. (1))	300	300 and 600	300	300
Maximum peak pressure used in the modelling (bar)	112	37 and 112 ^a	112	112
Work exchanger volume (L), V_b	40	40–500	40	40–500
Pipe internal diameter (mm) ^a	21.2	21.2–80	21.2	21.2–80
Pipe length incorporating recirculation pump (m) ^a	2.2	2.2–7.2	2.2	2.2–7.2

^a The length and diameter of the pipe in the recirculation loop was increased according to the number of membrane elements in series N_s . The length in the current prototype at University of Birmingham is 2.2 m with internal diameter of 21.2 mm. Consequently, we added 1 m to the pipe length for each additional membrane element of length 1 m. Standard pipe internal diameters of 21.2, 32, 44, 56, 68.3 and 80 mm were used for $N_s = 1, 2, 3, 4, 5$ and 6 elements in series, respectively. Peak pressure safety margin of 8 and 4 bar was considered for the XUS and XLE membranes respectively.

work exchanger when scaling up. In this study, we assume that the work exchanger is constructed from a pressure vessel similar to those used to house the RO membranes. Thus, we define the total internal volume V_{total} of all pressure vessels as:

$$V_{\text{total}} = V_b + V_h \quad (4)$$

where V_b is the volume of the work exchanger and V_h is the volume of the membrane housings (see Fig. 5). V_{total} is used as an indicator of system size. Then we define V_{total}/V_h as a parameter that varies from 1 in the semi-batch case (i.e., no work exchanger, $V_b = 0$, corresponding to minimum system size) to a maximum value that represents the batch RO case (corresponding to maximum system size). Hybrid semi-batch/batch RO lies anywhere between these two extremes.

Thus, Fig. 6 plots the effect of system size on SEC (normalised against semi-batch SEC) for brackish feed ($c_{\text{feed}} = 3000 \text{ mg/L}$) in cases of $N_s = 1$ and 4 membranes in series. It shows how energy efficiency improves with size. For example, at $r = 0.97$, increasing V_{total}/V_h from 1 to 3 decreases SEC dramatically (by 54 %) thus showing the advantage of hybrid over pure semi-batch RO. This advantage becomes even more pronounced as recovery increases. For example, at $V_{\text{total}}/V_h = 2$, the ratio of SEC/SEC_{sb} decreases from 0.69 to 0.54 when raising the recovery from 0.93 to 0.97 (see Fig. 6A). Nonetheless, increasing V_{total}/V_h above 3 yields little further benefit in decreasing SEC, suggesting that pure-batch RO is not advisable for high-recovery brackish water desalination.

Overall, Fig. 6 highlights a trade-off between a more compact design (i.e., smaller V_{total}/V_h) vs. higher energy efficiency. In other words, there is a trade-off involving capital cost vs operating cost. The suggested range of $V_{\text{total}}/V_h = 2$ to 3 corresponds to a work exchanger size of 1 to 2 times that of the membrane housing.

We note that Hosseini-pour et al. [41] recently investigated this trade-off by conducting experiments with two different work exchanger volumes (around 20 and 40 L) using the same prototype as in this study. Li [46] also provided theoretical evidence supporting these findings. He predicted that if the cylinder (i.e., the work exchanger in free-piston batch RO design) is removed from a proposed improved semi-batch RO design (i.e., the system returns to the standard semi-batch RO configuration) the energy consumption increases by 30 %. He also predicted about 2 % increase in energy consumption when the cylinder is oversized or undersized.

4.2. Effect of number of membranes in series, N_s

In this subsection, we use the model to investigate the effect of varying the number of membranes in series N_s from 1 to 6 while keeping $N_p = 1$ (i.e., without the use of parallel membrane elements). The recirculation flow (Q_r/Q_f) is optimised.

4.2.1. Brackish water feed

Fig. 7 compares the hydraulic SEC of the recirculation and supply pumps, as well as the total hydraulic and electrical SEC, at recirculation flows Q_r/Q_f from 2 to 8. Increasing N_s increases SEC but less so at low recirculation flows. Recirculation flow affects the recirculation pump SEC much more than the supply pump SEC. Thus, the hydraulic SEC of the supply pump remains within the range of 1.05–1.3 kWh/m³ while

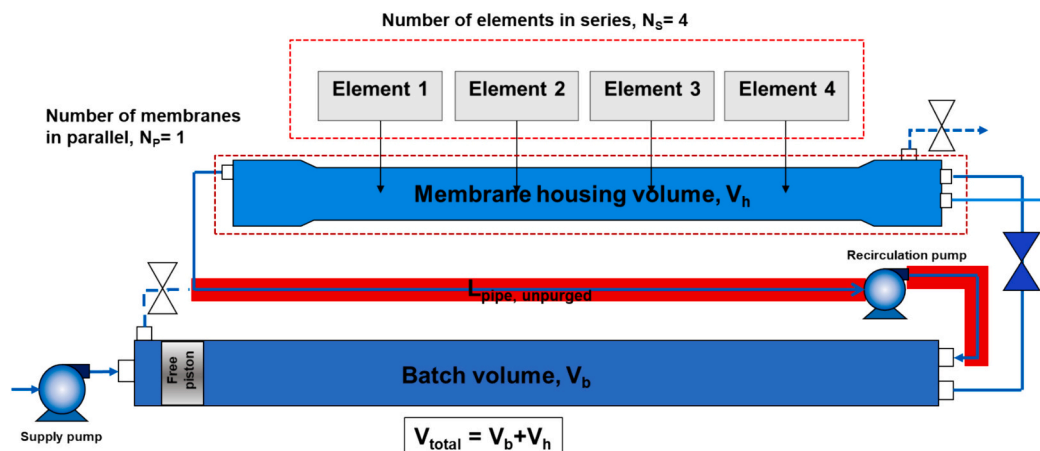


Fig. 5. Illustration of a free-piston batch RO system with labelled volumes. The red section highlights the pipeline length that remains unpurged during the flushing phase, resulting in higher salt retention and increased energy consumption.

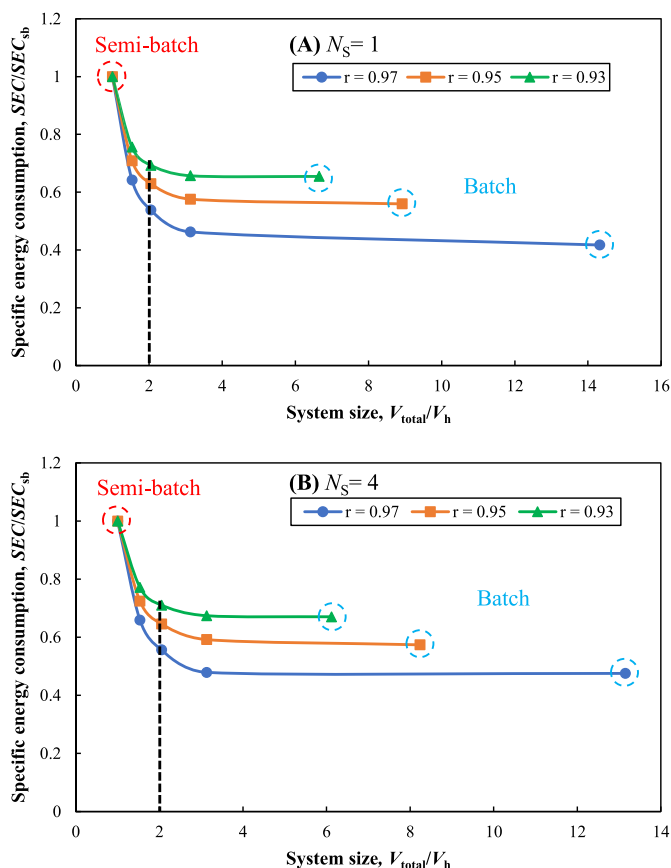


Fig. 6. Increasing work exchanger sizes increases system size but decreases energy consumption. Graph shows the effect of system size on SEC at three high recovery rates r , with $c_{feed} = 3000 \text{ mg/L}$, $Q_r/Q_f = 4$, and $J_w = 15 \text{ L/m}^2/\text{h}$ using XUS membrane. A) one membrane, and B) four membranes in series ($N_p = 1$ in all cases). Values are normalised against the semi-batch case, for which in A) $SEC_{sb} = 2.1, 1.5$ and 1.25 kWh/m^3 at recoveries of $r = 0.97, 0.95$, and 0.93 respectively; and $V_h \sim 40 \text{ L}$, and in B) $SEC_{sb} = 2.25, 1.62$ and 1.35 kWh/m^3 at recoveries of $r = 0.97, 0.95$, and 0.93 respectively; and $V_h \sim 150 \text{ L}$. Thus, $V_{total}/V_h = 2$ and 3 represent respectively work exchanger volumes of 40 and 80 L in A, and 160 and 320 L in B. Vertical dotted lines correspond to baseline cases in Table 1 above.

that of the recirculation pump increases from 0.02 to 1.4 kWh/m^3 , when $N_s = 6$. This trend is most pronounced at high values of $Q_r/Q_f \geq 6$. Nonetheless, when $N_s \leq 4$ and $Q_r/Q_f \leq 5$, the recirculation pump hydraulic SEC is $< 0.2 \text{ kWh/m}^3$ (see Fig. 7B), contributing only to a small fraction of the total hydraulic SEC. For example, when $N_s = 4$ and $Q_r/Q_f = 4$, the recirculation pump accounts for only 12.5% of the total hydraulic SEC. This minor impact on the energy efficiency of the batch RO system at very high recoveries during scale-up means that good performance can be maintained.

With $N_s \leq 2$, Q_r/Q_f has only a weak effect on overall SEC. This is because the increase in SEC of the recirculation pump is offset by the decreased SEC of the supply pump. However, operating at a higher Q_r/Q_f could help decrease the peak pressure (by about $10\text{--}15 \%$) and provide slightly better permeate quality (as shown in experimental results, see Table 3), while maintaining the SEC at a relatively consistent level. In contrast, with $N_s \geq 5$, operating at large recirculation flows ($Q_r/Q_f \geq 6$) has a greater impact on total SEC. Therefore, at $N_s \leq 3$, operation at Q_r/Q_f of 3 to 7 is recommended while for $N_s \geq 4$, it is better to operate at lower Q_r/Q_f (3 to 5) to minimize the SEC.

We also predict the total electrical SEC assuming 80% pump efficiency for both the recirculation and supply pumps as other modelling studies of batch RO [32,33,38]. With $Q_r/Q_f \leq 5$ and $N_s \leq 4$ at $r = 0.97$ (which is used later for the scale-up cases in Section 4.3), the total electrical SEC in brackish water is $< 1.6 \text{ kWh/m}^3$ (see Fig. 7D). Considering that the recirculation pump efficiency may be lower than that of the supply pump, we conducted a sensitivity analysis to evaluate its impact on the total electrical SEC. Sensitivity to the recirculation pump efficiency is minimal at small scale and low recirculation flow rates but becomes much more noticeable as the recirculation flow increases. Therefore, recirculation pump efficiency becomes crucial in the scale-up, as flow rate is much higher and the recirculation pump's energy consumption constitutes a larger share of the system's total energy use. As an example, at $Q_r/Q_f = 4$, when recirculation pump efficiency decreases from 80 to 50% , the total electrical SEC will increase by 5% and 11% when $N_s = 4$ and $N_s = 6$, respectively. The detailed analysis can be found in the SI Section 4.

On increasing the number of membranes and the recirculation flow, we increase the diameter of the piping and valves to keep the flow velocity in the pipe in a standard range (see Table 4 footnote). Thus, the pressure drop in valves and piping remains almost unchanged, but the membrane cross-flow pressure drop rises, particularly to a greater degree in the cases of $N_s \geq 5$ (see Fig. 8). Simultaneously, the recirculation pump is required to transfer much larger volumes of brine during refill, resulting in an increase in its energy consumption ($E = \int p_R \cdot dV_R$).

Fig. 8 also compares membrane friction pressure drop for thick (Fig. 8A) and thin (Fig. 8B) feed spacers, according to recirculation flow

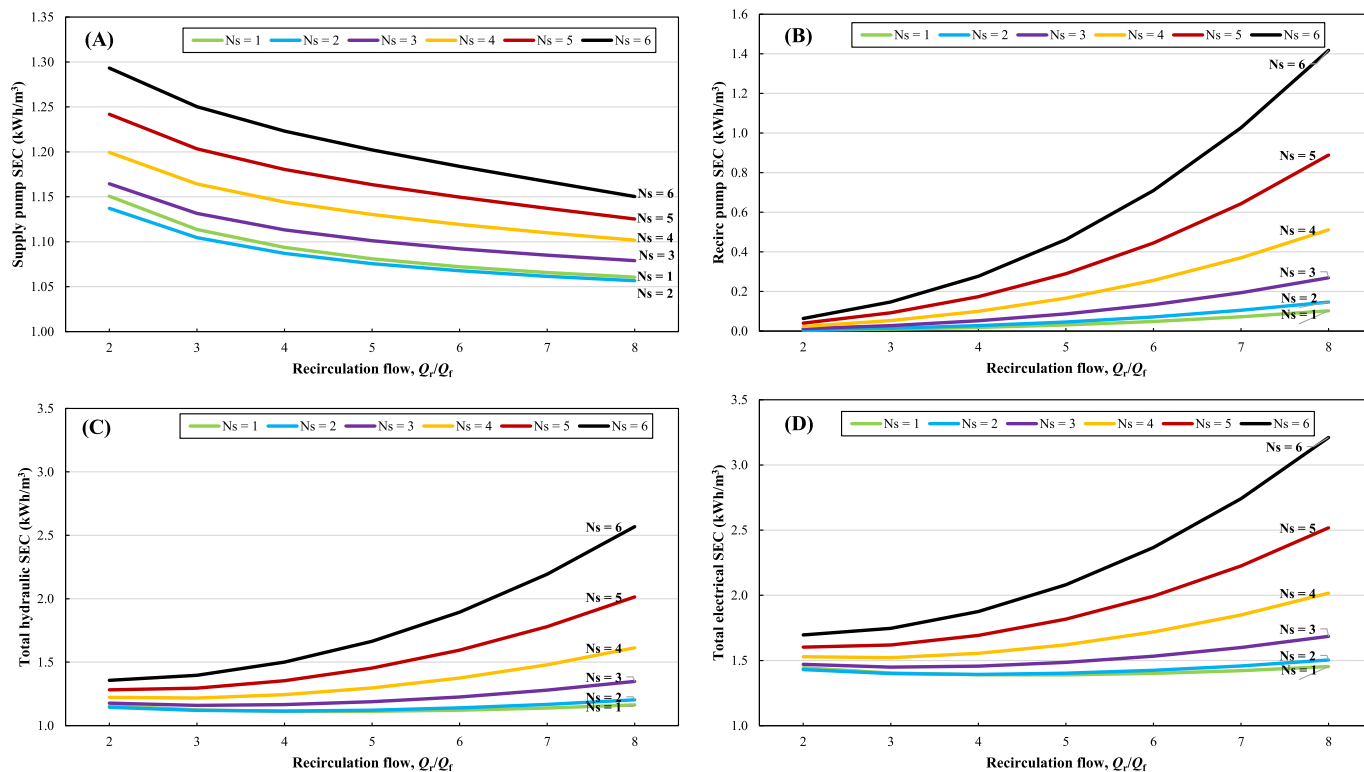


Fig. 7. SEC vs recirculation flow, according to number of membranes in series ($N_s = 1$ – 6), A) supply pump hydraulic SEC, B) recirculation pump hydraulic SEC, C) total hydraulic SEC, and D) total electrical SEC (assuming 80 % pump efficiency for recirculation and supply pumps). $N_p = 1$. Brackish water, $c_{feed} = 3000$ mg/L, $r = 0.97$, and $J_w = 15$ L/m²/h. Hybrid semi-batch/batch operation.

and the number of membranes in series. Both cases show a greater rise in membrane friction pressure drop when $N_s \geq 5$ and $Q_r/Q_f \geq 5$, with this trend being more pronounced with thin feed spacers. Conversely, when $Q_r/Q_f \leq 5$ and $N_s \leq 4$, the membrane pressure drop remains under 100 kPa for thick feed spacers and under 200 kPa for thin feed spacers.

4.2.2. Seawater feed

The trends with seawater resemble those with brackish water feed. As the osmotic pressure of seawater is much higher, however, the recovery is much lower than with brackish water ($r = 0.66$ down from 0.97). Thus, the initial semi-batch phase is not used in the seawater case. Because of the increased pressure, the supply pump SEC greatly exceeds the recirculation pump SEC. For example, when $N_s = 4$ and $Q_r/Q_f = 4$, the recirculation pump hydraulic SEC accounts for only 4.3 % of the total SEC. Therefore, increasing the Q_r/Q_f value has less impact on the total hydraulic SEC compared to the brackish water case. For instance, with four membranes in series ($N_s = 4$), increasing Q_r/Q_f from 2 to 8 results in only a 19 % increase in total hydraulic SEC compared to 48 % with brackish water. Even with $N_s = 5$, operation at high Q_r/Q_f such as 6 increases the hydraulic SEC by only 15 % compared to SEC at $Q_r/Q_f = 2$ (see Fig. 9C).

In the seawater case overall, SEC is insensitive to Q_r/Q_f up to $N_s = 3$. With $N_s \geq 4$ it is better to operate at $Q_r/Q_f \leq 6$ to avoid significant increase in SEC. With $Q_r/Q_f \leq 5$ and $N_s \leq 4$ at $r = 0.66$ (which is used later for the scale-up cases in Section 4.3), the total electrical SEC in seawater is < 3 kWh/m³ (see Fig. 9D).

4.3. Free-piston batch RO scale-up: design examples

In this subsection, we provide specific scale up examples based on a standard 16-in. diameter \times 4 m long pressure vessel as the work exchanger (giving a volume of $V_b = 500$ L) along with multiple RO elements in parallel.

We consider two case studies, the first using feed concentrations of 3000 mg/L (representing brackish water) and the second using 35,000 mg/L (representing seawater). We aim for maximum recovery, using either batch RO or hybrid semi-batch/batch RO as appropriate (see SI Section 3 for modelling of maximum recovery with brackish water). More details regarding main parameters such as recovery, flux, rejection and permeability are given in Table 4.

By considering a ratio of $V_{total}/V_h = 2$ (similar to the pilot used in [6,41]) and $V_{total}/V_h = 3$ (to minimize energy penalty by increasing the work exchanger volume as seen in Fig. 6), we estimate the required number of membranes. To accommodate these, we arrange them into several pressure vessels each containing 4 membranes in series.

4.3.1. Brackish water case study

When treating brackish water at $V_{total}/V_h = 2$, we initially estimated 13 RO membranes. Therefore, for practicality, we specify 12 membranes distributed across three pressure vessels connected in parallel (see Fig. 10A). At $V_{total}/V_h = 3$, 7 RO membranes were estimated. Thus, we specify 8 membranes accommodated in two parallel vessels (see Fig. 10B). Both arrangements are modelled for two different membrane types: (1) the XUS membrane, as assumed until now, and (2) the BW XLE-440 high-permeable brackish water RO element with membrane permeability of 4.6 L/m²/h/bar and pressure rating of 41 bar. The membrane permeabilities were experimentally verified in [40,41]. Also, the constants used to calculate membrane cross-flow pressure drop are $k = 300$ and 600 for the XUS and XLE respectively as explained in Section 3.1. The recirculation flow of $Q_r/Q_f = 4$ is chosen. To achieve high recovery, the system is operated in hybrid semi-batch/batch mode.

Based on the modelling, recovery is restricted by the pressure limit of the membranes (see SI Section 3). Thus, maximum recoveries of 0.93 and 0.97 are achievable for the XLE and XUS membranes respectively (see Table 5). In practice, recovery may be further restricted by the solubility of sparingly soluble salts in the feed, causing scaling.

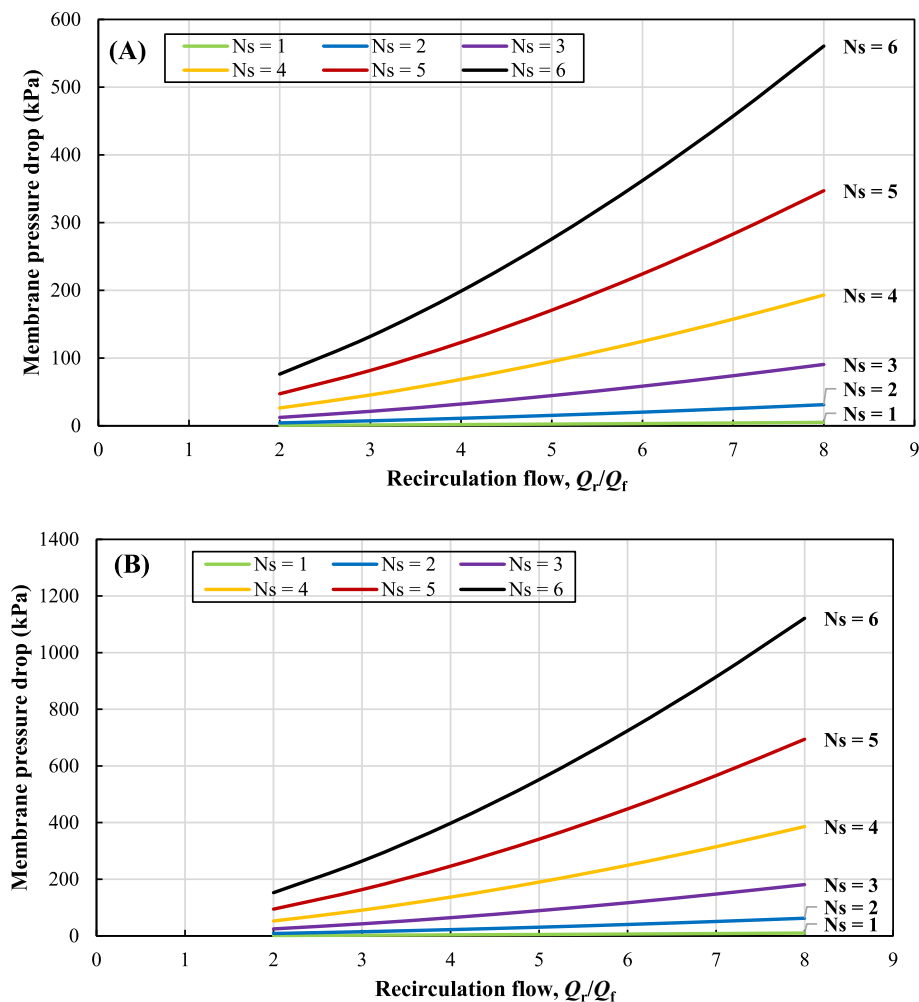


Fig. 8. Membrane cross-flow pressure drop as a function of recirculation flow at different number of membranes in series ($N_s = 1-6$, $N_p = 1$) A) thick feed spacer [$k = 300$], and B) thin feed spacer [$k = 600$]. Brackish water, $c_{\text{feed}} = 3000$ mg/L, $r = 0.97$, and $J_w = 15$ L/m²/h. Hybrid semi-batch/batch operation.

Nonetheless, recent studies have suggested that batch RO can avoid or delay scaling through mechanisms such as salinity cycling, osmotic backwash, flushing, and feed flow reversal [10,47].

The XLE membrane element has 30 % more active area than the XUS, giving more permeate output from the same number of elements. For example, in the case of using 12 elements, the total membrane area is 492 and 367.2 m² for XLE and XUS, giving a permeate output of 165 and 128 m³/day respectively (at recoveries of 0.93 and 0.97).

For the fixed work exchanger volume of $V_b = 500$ L, the use of fewer membranes (corresponding to increased V_{total}/V_h) decreases *SEC* but at the expense of decreased output. Thus, when $V_{\text{total}}/V_h = 2$, the total hydraulic *SEC* is 0.69 and 1.19 kWh/m³ for XLE and XUS respectively with outputs of 165 and 128 m³/day. But on increasing to $V_{\text{total}}/V_h = 3$, *SEC* decreases by 9 % for both types of membranes. However, this comes at the expense of a 34 % reduction in permeate output, which may not justify the modest energy saving (Table 5).

In the case of semi-batch RO ($V_{\text{total}}/V_h = 1$), we predict hydraulic *SEC* of 1.03 and 0.996 kWh/m³ when using 12 and 8 XLE membranes, respectively. In comparison, hybrid semi-batch/batch RO reduces *SEC* by 33 % ($V_{\text{total}}/V_h = 2$) and 37 % ($V_{\text{total}}/V_h = 3$). These reductions grow to 45 and 50 % respectively for the XUS membrane.

Key factors that restrict higher outputs include the maximum pressure rating of the membranes, which limits the flux. Additionally, if membrane permeability were greater, the peak pressure would decrease, allowing us to operate at higher fluxes without reaching the pressure limit. For instance, if the permeability of the XUS membrane

were 2 L/m²/h/bar instead of 0.8 L/m²/h/bar, flux could increase from 15 to 37.5 L/m²/h (assuming a maximum pressure of 112 bar). This would result in outputs of 320 m³/day and a hydraulic *SEC* of 1.735 kWh/m³ when using 12 membranes, translating to a 150 % increase in output and only a 45 % increase in *SEC*. These values underscore the critical role of membrane development in enhancing permeability and increasing burst pressure in the development and scale-up of batch RO.

An interesting observation also arises when comparing the *SEC* of the XLE membrane assuming the cross-flow pressure drop matches that of the XUS (i.e., assuming a constant value of $k = 300$ for the XLE instead of 600 in Eq. (1)). Then, the *SEC* would decrease even further, dropping from 0.69 to 0.567 kWh/m³ (an 18 % reduction) and from 0.628 to 0.506 kWh/m³ (a 19 % reduction) when using 12 and 8 elements, respectively. The *SEC* reduction could be even more substantial if we operated at higher fluxes or higher Q_r/Q_f ratios, as these adjustments would increase the pressure drop. This underscores the significance of membrane spacer development in minimizing *SEC* in batch RO.

Second law efficiency was also calculated using the equation for the thermodynamic minimum *SEC* provided in [5]. For the cases mentioned in Table 5, we determined the minimum *SEC* and divided it by the total electrical *SEC*. For the XLE membrane, the second law efficiency was 21.2 % and 23.3 % for cases with 12 and 8 modules, respectively. These values decreased to 15.8 % and 17.2 % for the XUS membrane due to its lower permeability and higher electrical *SEC* (though it has a better rejection and higher recovery rate). However, it still remains higher than existing brackish water RO systems, which typically exhibit second law

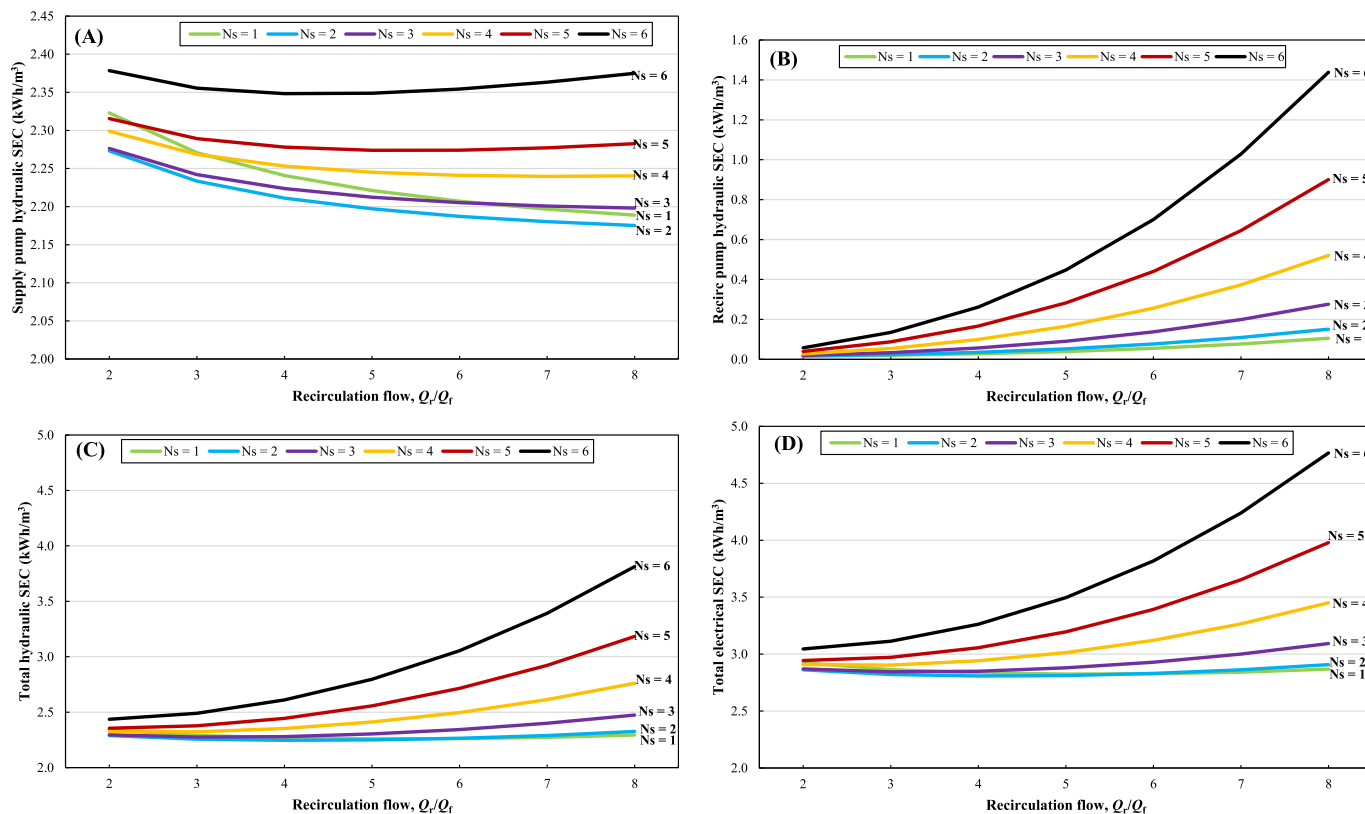


Fig. 9. SEC vs recirculation flow, according to number of membranes in series ($N_s = 1$ – 6), A) recirculation pump hydraulic SEC, B) supply pump hydraulic SEC, C) total hydraulic SEC, and D) total electrical SEC (assuming 80 % pump efficiency for recirculation and supply pumps). $N_p = 1$. Seawater, $c_{\text{feed}} = 35,000 \text{ mg/L}$, $r = 0.66$, and $J_w = 15 \text{ L/m}^2/\text{h}$, XUS membrane. Batch operation.

efficiencies ranging from 2 % to 15 % only [48].

Permeate output could be further increased by employing multiple independent systems in parallel. As an illustration, to obtain $1000 \text{ m}^3/\text{day}$ of permeate output about six systems using the XLE membrane would be needed. This approach may increase capital costs compared to conventional RO systems. Nonetheless, independent units may also improve reliability by providing backups.

4.3.2. Seawater case study

For the seawater case study, 12 membranes are used with three parallel pressure vessels giving $V_{\text{total}}/V_h = 2$ with V_b kept at 500 L, giving a recovery of 0.66 in batch mode (hybrid operation is avoided as this would lead to excess pressures). For maximum recovery, the high-pressure XUS membrane is used. The modelling results are summarised in Table 6.

With a peak pressure limit of 112 bar, we predict an output of $105 \text{ m}^3/\text{day}$ at a flux of $15 \text{ L/m}^2/\text{h}$. The hydraulic SEC is 2.371 kWh/m^3 , down by 13.1 % compared to 2.727 kWh/m^3 for semi-batch, and the electrical SEC is 2.963 kWh/m^3 . We can achieve a high recovery rate ($r = 0.66$), which is advantageous in applications with high salinity, such as mineral recovery, and the energy consumption is competitive with conventional seawater desalination. However, low membrane permeability and osmotic backflow are the primary obstacles to achieving even greater energy efficiency.

Although most studies [32,38] assumed permeability of $3 \text{ L/m}^2/\text{h}/\text{bar}$ in their modelling, we use the experimentally validated value of only $0.8 \text{ L/m}^2/\text{h}/\text{bar}$. If we were to assume 2 or $4 \text{ L/m}^2/\text{h}/\text{bar}$, hydraulic SEC would reduce to 2.023 and 1.907 kWh/m^3 respectively (down by 15 and 20 % from 2.371 kWh/m^3 at $0.8 \text{ L/m}^2/\text{h}/\text{bar}$). This would be accompanied by lower peak pressures of 102 and 98 bar respectively, allowing an increase in water flux and/or recovery if the same peak pressure were maintained. This, in turn, would increase permeate output. For instance,

at a permeability of $2 \text{ L/m}^2/\text{h}/\text{bar}$, flux could be increased from 15 to $29.4 \text{ L/m}^2/\text{h}$, boosting the permeate output to $207 \text{ m}^3/\text{day}$ at the cost of higher SEC of 2.656 kWh/m^3 . This corresponds to doubling the permeate output while the SEC increases only by 12 %. These findings again underline the potential for future enhancements in membrane permeability to enhance the energy efficiency and overall competitiveness of batch RO in high-pressure high-recovery seawater desalination, or other similar applications requiring a high concentration factor with saline feedwater.

Moreover, osmotic backflow is estimated at 4.5 L per element per cycle, i.e., 54 L for the 12-element system, resulting in a 12 % loss of permeate output. If this backflow were eliminated, we could achieve higher recoveries or lower SECs. For the brackish water case, osmotic backflow is much less significant because the cycles are longer and with larger output. For example, when using 12 XUS membranes with brackish water, osmotic backflow sacrifices only 1 % of the total output.

The corresponding second law efficiency for the case detailed in Table 6 was 43.4 %, significantly higher than the cases reported in the literature [49]. This efficiency is 2–3 times higher than the brackish water cases discussed in Table 5 because the feed salinity is much higher. Consequently, the impact of inefficiencies (such as membrane friction losses) in batch RO is much less.

While readily available 16-in. pressure vessels from the RO market are assumed in this study, further scale up may be achieved using other types of larger pressure vessels. Alternatively, large pressure vessels may be developed specifically for use in batch RO. This will likely depend on sufficient commercial uptake to justify investment in facilities and tooling for manufacturing.

5. Conclusions

A modelling and scale up study of batch RO has been conducted for

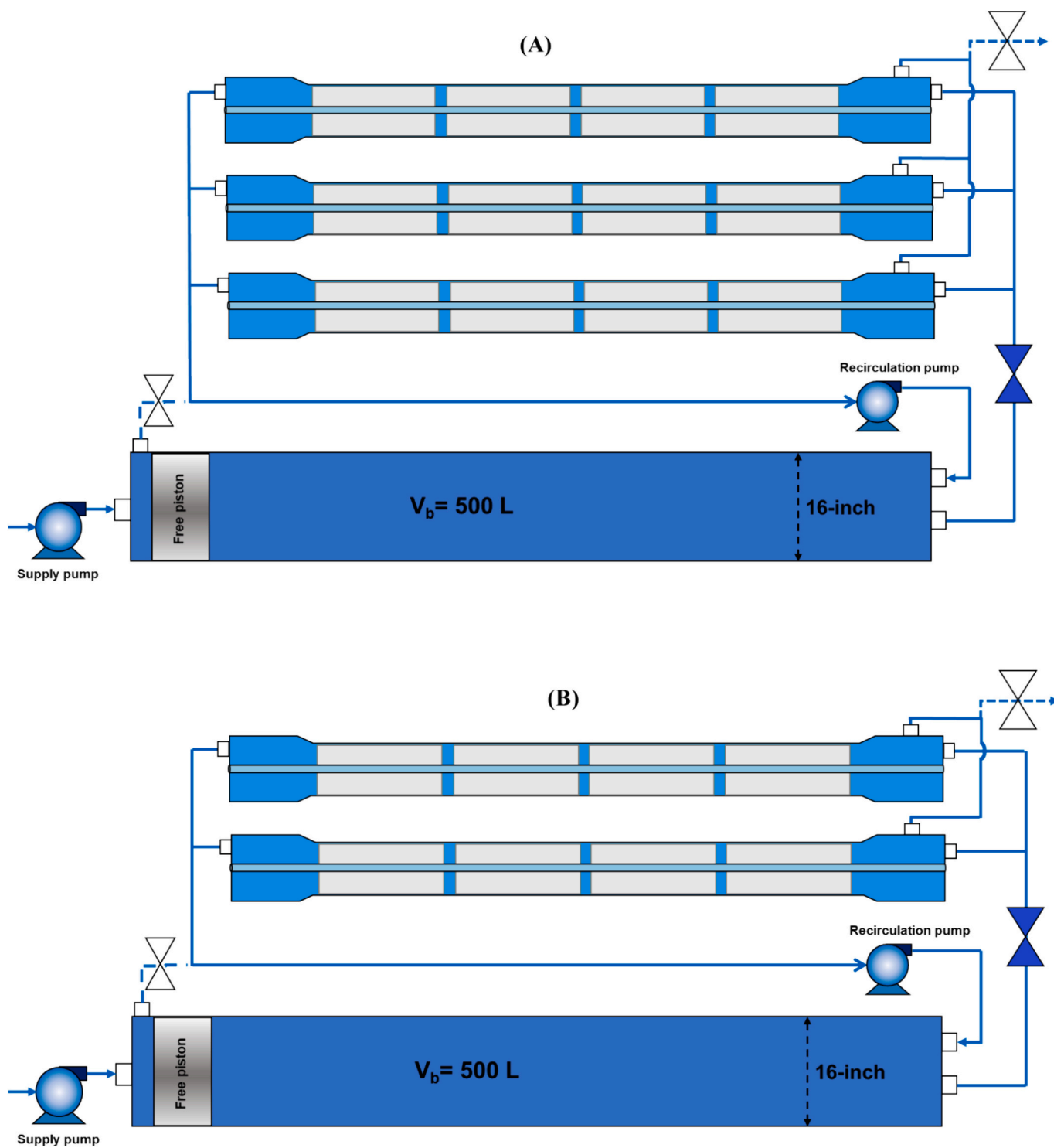


Fig. 10. Schematic of scaled-up free-piston batch RO configuration when using a 16-in. pressure vessel with a 4 m length as the work exchanger, for two cases: A) $V_{total}/V_h = 2$, requiring 12 membranes; B) $V_{total}/V_h = 3$, requiring 8 membranes.

brackish water and seawater feed represented respectively by 3000 mg/L and 35,000 mg/L NaCl solutions. Special attention has been paid to modelling the energy usage of the recirculation pump which becomes more significant as the number of membrane elements increases. Transmembrane water flux is set at 15 L/m²/h throughout. The key conclusions are:

1. Validation of the model against experiments shows agreement in SEC with error < 4 %.
2. Operating at up to 112 bar (i.e., safely below the 120 bar limit of the experimental system) the maximum possible recovery is 0.97 and 0.66 with brackish and seawater respectively.
3. For brackish water, hybrid semi-batch/batch operation is recommended whereas for seawater pure batch operation is recommended.
4. The volume of the work exchanger should be about 1 to 2× the volume of the membrane pressure vessels because this achieves significant (31–54 %) savings in SEC compared to semi-batch

Table 5

Details of a scaled up free-piston batch RO system using a 500 L work exchanger volume (a standard 16-in. diameter \times 4 m long pressure vessel) when treating brackish NaCl feed with concentration of $c_{\text{feed}} = 3000$ mg/L, at $J_w = 15$ L/m²/h and $Q_r/Q_f = 4$. Membrane permeability is adjusted to 0.8 and 4.6 L/m²/h/bar for XUS and XLE membranes respectively while rejection is set to 0.96 and 0.92 (consistent with experimental results [40,41]). The length and diameter of the pipe in the recirculation loop is 6.2 m and 56 mm respectively. Hybrid semi-batch/batch operation.

Feed conc. (mg/L), c_{feed}	Membrane type	V_{total}/V_h	No of elements	Total membrane area (m ²)	Recovery, r	Peak Pressure (bar)	Permeate output (m ³ /day)	Hydraulic SEC (kWh/m ³)			Electrical SEC (kWh/m ³)		
								Supply pump	Recirc pump	Total	Supply pump	Recirc pump	Total
3000	XLE	2	12	492	0.93	37	165	0.353	0.337	0.690	0.441	0.421	0.862
		3	8	328			108	0.339	0.289	0.628	0.424	0.361	0.785
	XUS	2	12	367.2	0.97	108	128	1.051	0.142	1.193	1.314	0.177	1.491
		3	8	244.8			84	0.98	0.114	1.094	1.225	0.142	1.367

Table 6

Details of a scaled up free-piston batch RO system using a 500 L work exchanger volume when treating NaCl feed concentration of 35,000 mg/L, representing seawater, at $J_w = 15$ L/m²/h, $Q_r/Q_f = 4$ (or recovery per pass of 0.2) and rejection of 0.98. The length and diameter of the pipe in the recirculation loop were assumed at 6.2 m and 56 mm respectively. Batch operation.

Feed conc. (mg/L), c_{feed}	Membrane type	V_{total}/V_h	No of elements	Total membrane area (m ²)	Recovery, r	Peak Pressure (bar)	Permeate output (m ³ /day)	Hydraulic SEC (kWh/m ³)			Electrical SEC (kWh/m ³)		
								Supply pump	Recirc pump	Total	Supply pump	Recirc pump	Total
35,000	XUS	2	12	367.2	0.66	112	105	2.227	0.143	2.371	2.784	0.179	2.963

where no work exchanger is used. Larger work exchanger volume further reduces SEC but only marginally.

- Arranging up to 4 membrane elements in series increases SEC only marginally (i.e., by <10 %) provided the recirculation flow does not exceed 4 \times the flow from the supply pump. With 5 or 6 elements in series, SEC becomes more sensitive to increased recirculation flow, but the electrical SEC can be maintained below 1.5 kWh/m³ with brackish water ($r = 0.97$) and 3 kWh/m³ with seawater ($r = 0.66$) at such high recoveries.
- Specific designs are proposed based on a 500-L work exchanger connected to parallel pressure vessels each housing four 8-in. membrane elements.
- For brackish water feed, three parallel vessels (i.e., 12 membrane elements) provide 165 m³/day and 128 m³/day of permeate output with XLE and XUS membranes respectively, achieving recoveries of 0.93 and 0.97 with hydraulic SEC of 0.69 and 1.19 kWh/m³. These values represent SEC reductions of 33 % and 45 % compared to semi-batch RO. Assuming an efficiency of 80 % for the supply and recirculation pumps, this translates to electrical SEC of 0.862 and 1.487 kWh/m³ for XLE and XUS membranes respectively.
- Using a similar arrangement of 12 XUS membranes for seawater, at $r = 0.66$, batch RO provides 105 m³/day permeate output, with hydraulic SEC of 2.37 kWh/m³ (a 13 % reduction compared to semi-batch) and electrical SEC of 2.962 kWh/m³.
- The second law efficiency of the scaled-up case study with seawater was 43.4 %, approximately twice as high as the brackish water case study, which reached up to 23.3 %. In the process of scaling up, the second law efficiency decreased but only slightly, by <5 %.
- Future high-permeability membranes (giving 2 L/m²/h/bar as compared to 0.8 L/m²/h/bar for the XUS) could enhance output by 150 % and 97 % with SEC penalty of 12 % and 45 % for brackish and seawater respectively, without exceeding the maximum pressure of 112 bar.

This study has been validated by means of a single-acting free-piston batch RO system. However, we expect that the trends of the results will apply also to other types of batch RO systems using pressurized vessels, such as double-acting systems or systems using bladders [30,50]. This is because these systems all work by similar principles.

Though outputs above 300 m³/day are difficult to achieve in a single unit using the suggested 16-in. pressure vessel as a work exchanger, larger outputs are possible using multiple units or custom-designed vessels to increase the work exchanger volume. In summary, while this work provides a solid foundation for scaling up free-piston batch RO systems, it does not set an upper limit on their size. Greater system sizes are conceivable, but addressing the challenges outlined in this study will require continued research, technological innovation, and comprehensive economic analysis.

Regarding future work, it is important to find efficient pumps specifically designed for the pressure variations in the batch RO process. Additionally, developing modules with lower cross-flow pressure drop is beneficial for scaling up batch RO. As mentioned in Section 4.2.1, pressure drop increases with system scale, impacting recirculation pump energy consumption. Exploring alternative pressure vessels for the work exchanger is also recommended. For example, adapting designs with larger diameters from other industries, or different geometries may provide alternatives beyond those available in the desalination market, permitting larger scale-up factors. A comprehensive techno-economic analysis is also needed to assess the cost-benefit ratio of scaling up batch RO systems. This should include evaluating capital costs, operational expenses, and potential savings in energy and maintenance compared to conventional continuous RO systems.

CRediT authorship contribution statement

E. Hosseinipour: Conceptualization, Formal analysis, Investigation, Methodology, Writing – original draft, Writing – review & editing. **P.A. Davies:** Conceptualization, Writing – review & editing, Supervision, Project administration, Funding acquisition.

Declaration of competing interest

The authors would like to declare that a spinout company (Salinity Solutions Ltd) has been formed to exploit the technology described in this article, and that one of the authors (PAD) has an equity stake in the spinout company.

Data availability

Data files are provided as supplementary documents.

Acknowledgements

This project has received funding from the Engineering and Physical Sciences Research Council, UK (Grant Ref: EP/T025867/1).

Appendix A. Supplementary data

Supplementary data to this article can be found online at <https://doi.org/10.1016/j.desal.2024.117980>.

References

- N. Ghaffour, T.M. Missimer, G.L. Amy, Technical review and evaluation of the economics of water desalination: current and future challenges for better water supply sustainability, *Desalination* 309 (2013) 197–207.
- F.E. Ahmed, A. Khalil, N. Hilal, Emerging desalination technologies: current status, challenges and future trends, *Desalination* 517 (2021) 115183.
- P.A. Davies, J. Wayman, C. Alatta, K. Nguyen, J. Orfi, A desalination system with efficiency approaching the theoretical limits, *Desal. Water Treat.* 57 (2016) 23206–23216.
- K. Park, P.A. Davies, A compact hybrid batch/semi-batch reverse osmosis (HBSRO) system for high-recovery, low-energy desalination, *Desalination* 504 (2021) 114976.
- E. Hosseiniour, S. Karimi, S. Barbe, K. Park, P.A. Davies, Hybrid semi-batch/batch reverse osmosis (HSBRO) for use in zero liquid discharge (ZLD) applications, *Desalination* 544 (2022) 116126.
- S. Karimi, R. Engstler, E. Hosseiniour, M. Wagner, F. Heinzler, M. Piepenbrink, S. Barbe, P. Davies, High-pressure batch reverse osmosis (RO) for zero liquid discharge (ZLD) in a Cr (III) electroplating process, *Desalination* 117479 (2024).
- P. Davies, A. Affi, F. Khatoun, G. Kuldip, S. Javed, S. Khan, Double-acting batch-RO system for desalination of brackish water with high efficiency and high recovery, in: *Desalination for the Environment—Clean Energy and Water*, Rome, 2016, pp. 23–25.
- K. Park, L. Burlace, N. Dhakal, A. Mudgal, N.A. Stewart, P.A. Davies, Design, modelling and optimisation of a batch reverse osmosis (RO) desalination system using a free piston for brackish water treatment, *Desalination* 494 (2020) 114625.
- E. Hosseiniour, K. Park, L. Burlace, T. Naughton, P.A. Davies, A free-piston batch reverse osmosis (RO) system for brackish water desalination: experimental study and model validation, *Desalination* 527 (2022) 115524.
- E. Hosseiniour, E. Harris, H.A. El Nazer, Y.M. Mohamed, P.A. Davies, Desalination by batch reverse osmosis (RO) of brackish groundwater containing sparingly soluble salts, *Desalination* 566 (2023) 116875.
- A.G. Capodaglio, A. Callegari, D. Ceconet, D. Molognoni, Sustainability of decentralized wastewater treatment technologies, *Water Pract. Technol.* 12 (2017) 463–477.
- A. Hafeez, Z. Shamair, N. Shezad, F. Javed, T. Fazal, S. Ur Rehman, A.A. Bazmi, F. Rehman, Solar powered decentralized water systems: a cleaner solution of the industrial wastewater treatment and clean drinking water supply challenges, *J. Clean. Prod.* 289 (2021) 125717.
- V.G. Varma, S. Jha, L.H.K. Raju, R.L. Kishore, V. Ranjith, A review on decentralized wastewater treatment systems in India, *Chemosphere* 300 (2022) 134462.
- N. Jahan, M. Tahmid, A.Z. Shoronika, A. Fariha, H. Roy, M.N. Pervez, Y. Cai, V. Naddeo, M.S. Islam, A comprehensive review on the sustainable treatment of textile wastewater: zero liquid discharge and resource recovery perspectives, *Sustainability* 14 (2022) 15398.
- Z. Lv, H. Feng, R. Chen, B. Shen, H. Tao, Y. Ding, Y. Xia, Y. He, Y. Zhang, Simultaneous removal of fluorine and dissolved silica from semiconductor wastewater by an in-situ crystal nucleation method towards near-zero liquid discharge, *Desalination* 117831 (2024).
- G. Mekuria, Dairy wastewater treatment through synergies of the biological and hybrid membrane: a systematic review, *J. Environ. Inform. Lett* 8 (2022) 31–50.
- A. Bottino, G. Capannelli, A. Comite, C. Costa, R. Firpo, A. Jezowska, M. Pagliero, Treatment of olive mill wastewater through integrated pressure-driven membrane processes, *Membranes* 10 (2020) 334.
- B. Martin-Gorriz, J.F. Maestre-Valero, B. Gallego-Elvira, P. Marín-Membrive, P. Terrero, V. Martínez-Alvarez, Recycling drainage effluents using reverse osmosis powered by photovoltaic solar energy in hydroponic tomato production: environmental footprint analysis, *J. Environ. Manag.* 297 (2021) 113326.
- N. van Linden, R. Shang, G. Stockinger, B. Heijman, H. Spanjers, Separation of natural organic matter and sodium chloride for salt recovery purposes in zero liquid discharge, *Water Res. Indust.* 23 (2020) 100117.
- X. Liu, J. Ma, E. Li, J. Zhu, H. Chu, X. Zhou, Y. Zhang, Multistage membrane-integrated zero liquid discharge system for ultra-efficient resource recovery from steel industrial brine: pilot-scale investigation and spatial membrane fouling, *J. Membr. Sci.* 699 (2024) 122655.
- A. Panagopoulos, V. Giannika, Decarbonized and circular brine management/valorization for water & valuable resource recovery via minimal/zero liquid discharge (MLD/ZLD) strategies, *J. Environ. Manag.* 324 (2022) 116239.
- A. Khalil, S. Mohammed, R. Hashaikeh, N. Hilal, Lithium recovery from brine: recent developments and challenges, *Desalination* 528 (2022) 115611.
- P. Goh, K. Wong, A. Ismail, Membrane technology: a versatile tool for saline wastewater treatment and resource recovery, *Desalination* 521 (2022) 115377.
- J. Du, T.D. Waite, P. Biesheuvel, W. Tang, Recent advances and prospects in electrochemical coupling technologies for metal recovery from water, *J. Hazard. Mater.* 442 (2023) 130023.
- G. Naidu, L. Tijing, M.A. Johir, H. Shon, S. Vigneswaran, Hybrid membrane distillation: resource, nutrient and energy recovery, *J. Membr. Sci.* 599 (2020) 117832.
- D.-G.f.R.a.I. European Commission, Horizon Europe Strategic Plan 2025–2027, 2024, <https://doi.org/10.2777/092911>.
- M. Li, Y. Heng, J. Luo, Batch reverse osmosis: a new research direction in water desalination, *Sci. Bull.* 65 (2020) 1705–1708.
- M. Li, Effects of finite flux and flushing efficacy on specific energy consumption in semi-batch and batch reverse osmosis processes, *Desalination* 496 (2020) 114646.
- A. Das, D.M. Warsinger, Batch counterflow reverse osmosis, *Desalination* 507 (2021) 115008.
- Q.J. Wei, C.I. Tucker, P.J. Wu, A.M. Truworthly, E.W. Tow, Impact of salt retention on true batch reverse osmosis energy consumption: experiments and model validation, *Desalination* 479 (2020) 114177.
- T. Qiu, P.A. Davies, Comparison of configurations for high-recovery inland desalination systems, *Water* 4 (2012) 690–706.
- J.R. Werber, A. Deshmukh, M. Elimelech, Can batch or semi-batch processes save energy in reverse-osmosis desalination? *Desalination* 402 (2017) 109–122.
- J. Swaminathan, E.W. Tow, R.L. Stover, Practical aspects of batch RO design for energy-efficient seawater desalination, *Desalination* 470 (2019) 114097.
- M. Li, N. Chan, J. Li, Novel dynamic and cyclic designs for ultra-high recovery waste and brackish water RO desalination, *Chem. Eng. Res. Des.* 179 (2022) 473–483.
- Z. Gal, A. Efraty, CCD series no. 18: record low energy in closed-circuit desalination of ocean seawater with nanoH₂O elements without ERD, *Desalin. Water Treat.* 57 (2016) 9180–9189.
- A. Efraty, Closed circuit desalination series no-4: high recovery low energy desalination of brackish water by a new single stage method without any loss of brine energy, *Desalin. Water Treat.* 42 (2012) 262–268.
- H. Gu, M.H. Plumlee, M. Boyd, M. Hwang, J.C. Lozier, Operational optimization of closed-circuit reverse osmosis (CCRO) pilot to recover concentrate at an advanced water purification facility for potable reuse, *Desalination* 518 (2021) 115300.
- A. Das, A.K. Rao, S. Alnajdi, D.M. Warsinger, Pressure exchanger batch reverse osmosis with zero downtime operation, *Desalination* 574 (2024) 117121.
- H. Abu Ali, M. Baronian, L. Burlace, P.A. Davies, S. Halasah, M. Hind, A. Hossain, C. Lipchin, A. Majali, M. Mark, Off-grid desalination for irrigation in the Jordan Valley, *Desal. Water Treat.* 168 (2019) 143–154.
- E. Hosseiniour, P. Davies, Effect of membrane properties on the performance of batch reverse osmosis (RO): the potential to minimize energy consumption, *Desalination* 577 (2024) 117378.
- E. Hosseiniour, P. Davies, Direct experimental comparison of batch reverse osmosis (RO) technologies, *Desalination* 117717 (2024).
- R. Zhao, S. Porada, P. Biesheuvel, A. Van der Wal, Energy consumption in membrane capacitive deionization for different water recoveries and flow rates, and comparison with reverse osmosis, *Desalination* 330 (2013) 35–41.
- A. Haidari, S. Heijman, W. van der Meer, Visualization of hydraulic conditions inside the feed channel of reverse osmosis: a practical comparison of velocity between empty and spacer-filled channel, *Water Res.* 106 (2016) 232–241.
- B. Massey, *Mechanics of Fluids 4*, 4th edition, The English Language Book Society, 1980.
- D.W. Solutions, Filmtec™ reverse osmosis membranes, *Technical Man. Form 399* (2010) 1–180.
- M. Li, Effect of cylinder sizing on performance of improved closed-circuit RO (CCRO), *Desalination* 561 (2023) 116688.
- D.M. Warsinger, E.W. Tow, L.A. Maswadeh, G.B. Connors, J. Swaminathan, Inorganic fouling mitigation by salinity cycling in batch reverse osmosis, *Water Res.* 137 (2018) 384–394.
- J.H. Lienhard, G.P. Thiel, D.M. Warsinger, L.D. Banchik, Low carbon desalination: status and research, development, and demonstration needs, in: Report of a Workshop Conducted at the Massachusetts Institute of Technology in Association With the Global Clean Water Desalination Alliance, 2016.
- J. Kim, K. Park, D.R. Yang, S. Hong, A comprehensive review of energy consumption of seawater reverse osmosis desalination plants, *Appl. Energy* 254 (2019) 113652.
- S. Cordoba, A. Das, J. Leon, J.M. Garcia, D.M. Warsinger, Double-acting batch reverse osmosis configuration for best-in-class efficiency and low downtime, *Desalination* 506 (2021) 114959.